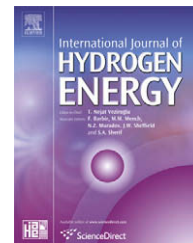


Available at www.sciencedirect.comjournal homepage: www.elsevier.com/locate/he

Linear sweep voltametry studies on oxygen reduction of some oxides in alkaline electrolytes

M.V. Ananth^{a,*}, V.V. Giridhar^b, K. Renuga^c

^aNi-MH Section, Electrochemical Power Sources Division, Central Electrochemical Research Institute, Karaikudi, 630 006 Tamil Nadu, India

^bElectrodics and Electrocatalysis (EEC) Division, Central Electrochemical Research Institute, Karaikudi, 630 006 Tamil Nadu, India

^cDepartment of Chemistry, Thiagarajar College, Madurai 625 009, India

ARTICLE INFO

Article history:

Received 7 April 2008

Received in revised form

21 October 2008

Accepted 5 November 2008

Published online ■

Keywords:

Oxygen reduction reaction

Electrocatalytic oxides

Bifunctional air electrodes

Discharge capacity

Linear sweep voltametry

ABSTRACT

The study uses linear sweep voltametry (LSV) to observe the efficiency of oxygen reduction on some oxides and their mixtures in 6 M KOH at 25 °C. The investigated materials are Ag₂O, MnO₂, Sm₂O₃, Dy₂O₃ and NdO₂. The electrocatalytic oxygen reduction reactions (ORR) on Teflon-bonded, oxide + graphite electrodes are studied. The oxygen reduction potentials for electrodes containing these materials as catalyst are seen as –60.67, –270.31, –111, –159.58 and –130.24 mV, respectively. Mixture combinations of these oxides give a higher ORR peak current thereby showing evidence of synergetic effect. Air–MH cells using some of the above investigated oxides as catalyst for air electrode are constructed and studied. Best performance is obtained with silver oxide. The LSV findings are in accordance with air–MH cell charge/discharge experiments and for best performance prefer shift of the ORR onset potential to more positive positions.

© 2008 International Association for Hydrogen Energy. Published by Elsevier Ltd. All rights reserved.

1. Introduction

Several metallic oxides are known to exhibit superior electrochemical activity for at least one of the electrolysis, energy storage and/or fuel cell reactions. The ORR is involved in a number of electrochemical processes, such as metal corrosion, water electrolysis, and energy conversion/storage [1–3] and has been in limelight in recent decades [4]. Several materials are attracting interest in this regard. For example, the ORR on carbon-based electrodes has been extensively studied with different types of carbon materials like carbon black composites [5], highly oriented pyrolytic graphite (HOPG) [6], glassy carbon (GC) [7], boron-doped diamond (BDD) [8], reticulated vitreous carbon (RVC) [9] carbon nanotubes (CNT) [10], carbon nanofibers [11] and Ordered mesoporous carbon (OMC) [12] etc.

Renewable energy sources are attracting current interest for future energy requirements and for reducing carbon dioxide emission [13,14]. Polymer electrolyte membrane fuel cell (PEMFC) is a promising technology to convert stored renewable energy sources like hydrogen into electricity. One of the main factors which limit the widespread commercialization of PEMFC's is the cost of the cathode catalyst. The high cost is mainly due to the use of Pt as the catalyst for ORR. Great efforts have been made to reduce the amount of required Pt loading or even to replace Pt by non-noble metal catalysts [15–20].

Direct methanol fuel cell (DMFC) is one of the most promising options for mobile power source because of its high energy conversion efficiency and low pollutant emission [21,22]. Slow kinetics of ORR at the cathode of DMFCs is a serious problem [23,24]. Correspondingly a large number of

* Corresponding author. Tel.: +91 4565 227555; fax: +91 4565 227713.

E-mail address: mvananth@rediffmail.com (M.V. Ananth).

0360-3199/\$ – see front matter © 2008 International Association for Hydrogen Energy. Published by Elsevier Ltd. All rights reserved.
doi:10.1016/j.ijhydene.2008.11.002

investigations are being made to increase the ORR performance by using highly active electrocatalysts. It is, therefore, worthwhile to investigate at replacement of Pt by more abundant transition metals such as Fe, Co, Cu, Mn, Mo for multielectron transfer catalysis [25]. Development of suitable ethanol tolerant oxygen reduction electrocatalysts for direct ethanol fuel cells is also receiving interest [26].

Secondary metal–air batteries are promising power sources for portable electric devices or electric vehicles due to their high theoretical (e.g., 1085 Wh kg⁻¹ for a Zn–air battery) as well as practical (60–150 Wh kg⁻¹ for a Zn–air battery) specific energies, and also due to the low cost and low toxicity of the materials involved [27]. The development of this type of battery is, however, delayed for viable bifunctional air electrode in alkaline electrolytes.

In recent years, air–metal hydride system has attracted substantial attention [28–30] with initiations in metal hydride fuel cells [31]. The end of the battery life is determined by the cycle life of the air electrode. The use of bifunctional air electrodes that are less sensitive to corrosion is, therefore, demanded for a necessary increase of the cycle lifetime. The materials used as the bifunctional catalyst and the carbon support material greatly influence the lifetime of the air-electrode. Various types of electrocatalysts, e.g., Pt and Pt–Ru alloys have been investigated as a key component of the electrodes, but they are expensive. Significant progress has been made in recent years in the development of less expensive electrocatalysts such as perovskite, spinels, pyrochlores, other oxides, pyrolyzed macrocycles, etc. Among the alternatives for platinum catalysts, MnO₂ shows some promise of success due to its low cost and its high catalytic activity for the oxygen reduction [32]. The performance of air electrode composed of KMnO₄ catalyst for oxygen reduction reaction has also been examined [33]. Some studies have appeared in literature on its oxygen reduction characteristics [34,35]. Burchardt has evaluated the electrocatalytic activity and stability for air electrodes [36]. Linear sweep voltametry has been used to characterize oxygen reduction kinetics in alkaline solution on catalysts like platinum electrodes [37]. All that mentioned above point towards the importance of oxygen reduction catalysts Table 1. Thus, many efforts are addressed for the improvement in oxygen reduction kinetics in such catalysts. Several materials inclusive of rare earth based oxides [38] are available for such use. However, detailed studies are required to identify the best catalytic materials

with thorough characterisation of oxygen reduction reaction. Hence, this work is intended to investigate the efficiency of oxygen electroreduction on potential materials – Ag₂O, MnO₂, Sm₂O₃, Dy₂O₃ and NdO₂ – and some of their combinations with linear sweep voltametry in 6 M KOH solution along with some for use in bifunctional air electrodes.

2. Experimental

The catalyst (0.1 g) was mixed with an equal amount of KS44 graphite powder and sufficient quantity of PTFE and compacted over nickel foam at 5×10^3 kg cm⁻² for 3 min followed by heat treatment at 120 °C for 1 h under normal conditions for LSV measurements. To measure the ORR onset potentials of different catalytic samples LSV was performed with EG & G PAR Electrochemical system model 273 A in a standard three compartment cell in 6 M KOH under oxygen bubbling. A platinum clump was used as the counter electrode and an Hg/HgO reference electrode was used for all measurements. All the potentials were reported versus this reference electrode. Electrochemical cycling was done prior to LSV measurements at a scan rate of 100 mV/sec. All chemicals were Merck G. R. reagents. All measurements were made at 25 °C (with an accuracy of 0.05 °C) using a water thermostat. To make the results reproducible and reliable, a fresh electrolyte solution was used in every measurement.

Air electrodes for performance evaluation were produced in two layers: the catalyst layer on the electrolyte side and a hydrophobic diffusion layer on the gas side. The active layer contained a catalyst (typically 40 wt%), KS44 graphite powder (45 wt%) and PTFE (15 wt%). In this part we used different types of oxide catalysts namely Ag₂O, MnO₂, Sm₂O₃, Dy₂O₃ and NdO₂. All the investigated materials were of commercial AR grade variety. The graphite powder and the binder were ground and mixed together using isopropyl alcohol as dispersing agent and dough was obtained by adding PTFE. This dough was coated on one of the sides, and similarly another dough was prepared containing graphite and the active material and were ground and mixed together using isopropyl alcohol and a dough was obtained by adding PTFE and this was coated on the other side. Then the electrode was compacted at a pressure of 5×10^3 kg cm⁻² for 3 min followed by heat treatment at 120 °C for 1 h under normal conditions. The geometric area of the positive electrode was $2 \times 2.5 \times 2.5$ cm².

The composition of the alloy used for Air–MH cell assembly was Mm Ni_{3.48}Co_{0.73}Mn_{0.34}Al_{0.23}Fe_{0.02}Mo_{0.01}. The alloy was produced at DMRL, Hyderabad in collaboration with CECRI, Karaikudi. It was prepared by arc melting followed by necessary treatments and after annealing crushed mechanically into powder (<75 μm). A total of 8 g of MH alloy was mixed with 20% KS44 graphite powder, 10% carbonyl nickel and 10% silver oxide. PTFE was used as binder and the active material paste was applied over the foam substrate. Subsequently compaction was done at 5×10^3 kg cm⁻² for 3 min to obtain the metal hydride electrode followed by heat treatment at 120 °C for 1 h under normal conditions. The geometric area of the negative electrode was $2 \times 2.5 \times 2.5$ cm² and the thickness was 1.5 mm.

Table 1 – LSV parameters of investigated oxygen reduction catalysts.

Catalyst	Purging Details	Oxygen Reduction Potentials (mV)
Ag ₂ O	O ₂ – 15 min	–60.67
MnO ₂	O ₂ – 15 min	–270.31
Sm ₂ O ₃	O ₂ – 15 min	–111.00, –515.05
NdO ₂	O ₂ – 15 min	–130.24
Dy ₂ O ₃	O ₂ – 15 min	–158.58, –536.50
Ag ₂ O–MnO ₂	O ₂ – 15 min	–126
Ag ₂ O–Sm ₂ O ₃	O ₂ – 15 min	156.8, –56.86
Ag ₂ O–Dy ₂ O ₃	O ₂ – 15 min	122.42, –164.82

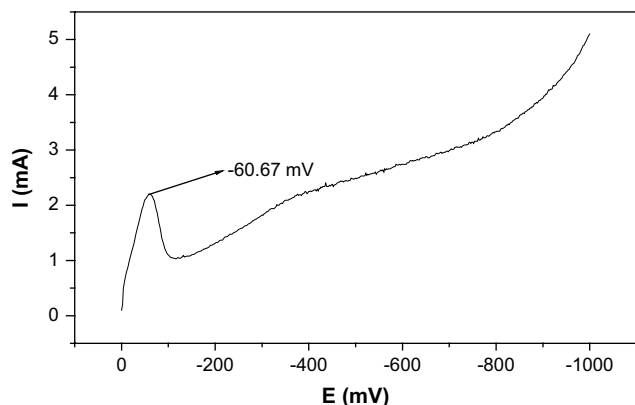


Fig. 1 – Linear sweep voltammogram with Ag_2O as catalyst.

The air electrode (cathode) and the metal hydride electrode (anode) were assembled and sealed in a prismatic container as reported previously [39]. Subsequently, the cell was subjected to formation cycles after soaking in 30% KOH solution. After the completion of formation cycles, the cells were charged at 500 mA for 6 h and discharged at 10 mA after a rest for 10 min in the case of engaging Ag_2O as electrocatalyst. In other cases, the cells were charged at 25 mA for 6 h and discharged at 10 mA after a rest for 10 min. The life cycling of the cells were studied using a 'Bitrode' LCN Battery Testing System at room temperature.

3. Results and discussions

3.1. LSV measurements

LSV measurements were made on the investigated materials for oxygen reduction reaction and the results are summarized in Table 1. The detailed discussions on the results are presented in the following sections.

3.1.1. LSV measurements on silver oxide

Silver based catalysts are well known and have an extensive history for use in alkaline electrolytes [40,41]. LSV curves for

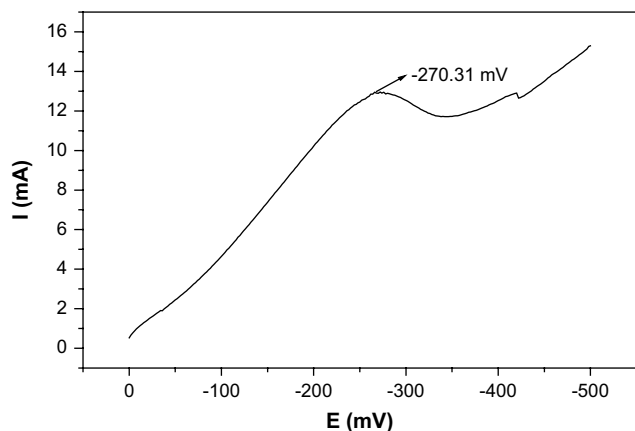


Fig. 2 – Linear sweep voltammogram with MnO_2 as catalyst.

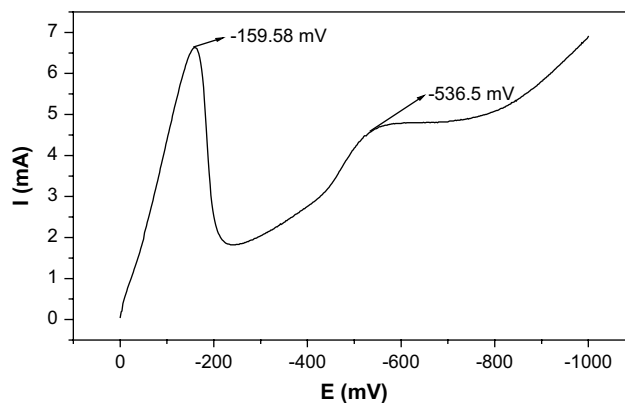


Fig. 3 – Linear sweep voltammogram with Dy_2O_3 as catalyst.

Ag_2O are given in Fig. 1. The oxygen reduction potentials for the Ag_2O electrode are observed around -61 mV. Even though oxygen reduction is known to proceed through at least two pathways [42], the two-electron pathway which involves an initial reduction reaction to produce H_2O_2 , and the H_2O_2 further reduce to OH^- or the decomposition of peroxide is applicable to metal oxides [43]. The improved activity could partly be attributed to relatively high activity for the O_2 reduction and the occurrence of an ORR mechanism via 4 electrons with Ag [44]. The pathway of oxygen reduction is strongly dependent on the electrode material. The optimum surface chemistry and bulk crystal structure is responsible for the observed superior oxygen reduction capabilities. This is in agreement with the observations of Zheng et al [45] who have reported that preservation of crystalline structures and existence of the extra surface oxygen-containing groups improve the ORR.

From curves in Figs. 1–8, one can see the ORR onset reduction potential of Ag_2O to be more positive than that of the other investigated samples. It is believed that the different ORR onset reduction potentials are caused by the differences in the surface activation and the more positive ORR onset reduction potential of Ag_2O reveals it to be more active amongst the studied samples. This may be partly aided by the fact that due to electrochemical operation the chemical composition is changed as reported by Wagner et al [41].

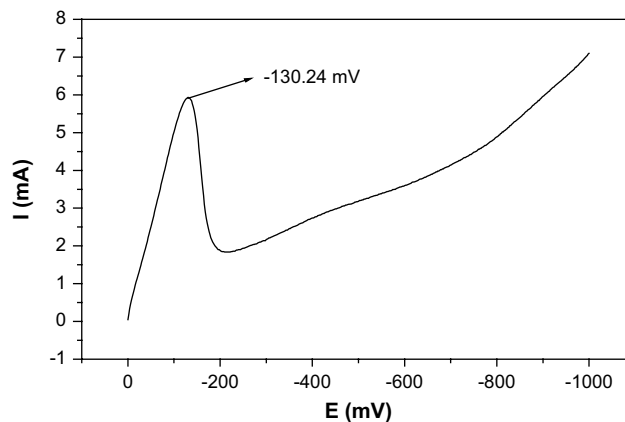


Fig. 4 – Linear sweep voltammogram with NdO_2 as catalyst.

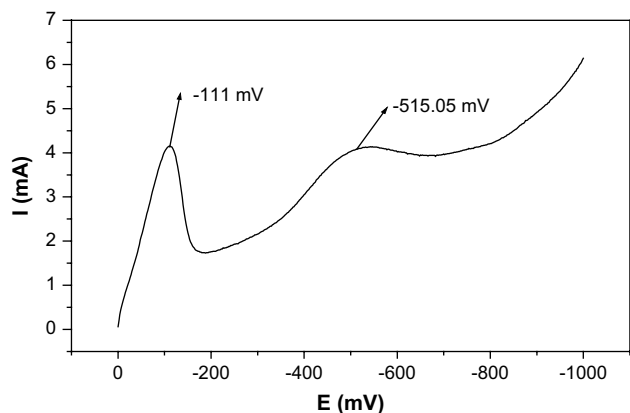


Fig. 5 – Linear sweep voltammogram with Sm_2O_3 as catalyst.

3.1.2. LSV measurements on manganese dioxide

Manganese oxides have been extensively studied and it has been stated that the activity of these catalysts is dependent on the kind of oxides [40]. LSV curves for MnO_2 are given in Fig. 2. The oxygen reduction potential for the MnO_2 electrode is seen at -270.31 mV. One of the functions of this oxide is to perform the decomposition of hydrogen peroxide, which is formed during the electrochemical reduction of oxygen by a disproportionation mechanism conducting the ORR to follow the complete reduction pathway, where a $4e^-$ transfer per oxygen molecule is obtained [33]. However, the inference is that due to these high negative values of oxygen reduction potentials, MnO_2 may not be a suitable material for use in air electrode. Results indicate that the reaction proceeds through the peroxide route and that the adjoining graphite matrix may also contribute to the catalysis of the ORR. However, the activity and mechanism by which the ORR takes place in MnO_2 is yet to be fully explored [46].

3.1.3. LSV measurements on dysporium oxide

LSV curves for Dy_2O_3 are given in Fig. 3. The oxygen reduction potentials are seen around -159 and -536 mV. The inference is that due to these high negative values of oxygen reduction

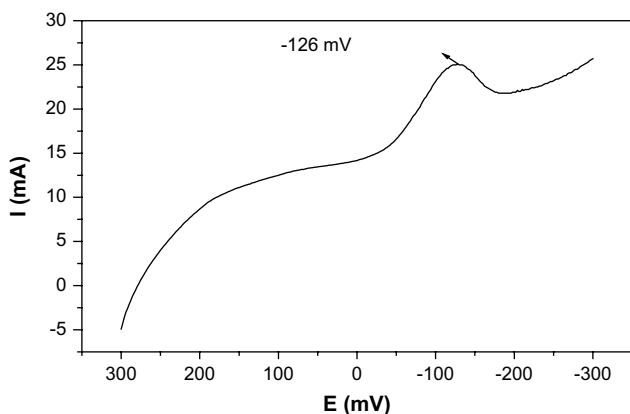


Fig. 6 – Linear sweep voltammogram with $\text{Ag}_2\text{O-MnO}_2$ mixture as catalyst.

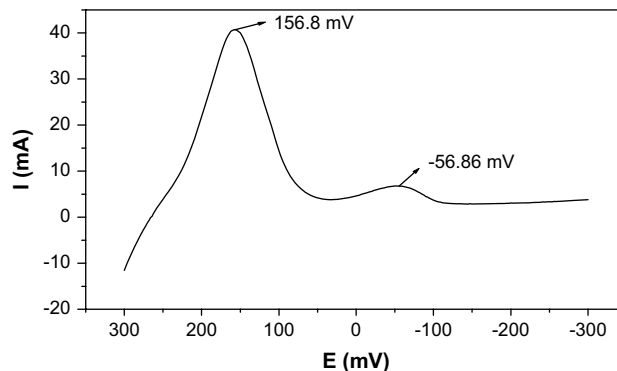


Fig. 7 – Linear sweep voltammogram with $\text{Ag}_2\text{O-Sm}_2\text{O}_3$ mixture as catalyst.

potentials, Dy_2O_3 may not be a suitable material for use in air electrode. The observed highly negative oxygen reduction potentials could be due to inhibition of oxygen reduction by the presence of hydrous oxides on the surface as is the case seen earlier with Pt based catalysts [47]. Moreover, the increase of over potential on cathodic side is not desirable for the intended application.

3.1.4. LSV measurements on neodymium oxide electrode

LSV curves for NdO_2 are given in Fig. 4. The oxygen reduction potentials are seen around -130 mV. The inference is that due to these high negative values of oxygen reduction potentials, NdO_2 also may not be a suitable material for use in air electrode.

3.1.5. LSV measurements on samarium oxide electrode

LSV curves for Sm_2O_3 are given in Fig. 5. The oxygen reduction potentials are seen around -111 and -515 mV, etc. The inference is that due to these high negative values of oxygen reduction potentials, Sm_2O_3 also may not be a suitable material for use in air electrode.

3.1.6. LSV measurements on oxide mixtures

LSV curves for some mixture combinations of some of the above investigated materials were done. $\text{Ag}_2\text{O-MnO}_2$, $\text{Ag}_2\text{O-Sm}_2\text{O}_3$, and $\text{Ag}_2\text{O-Dy}_2\text{O}_3$ were explored for oxygen reduction

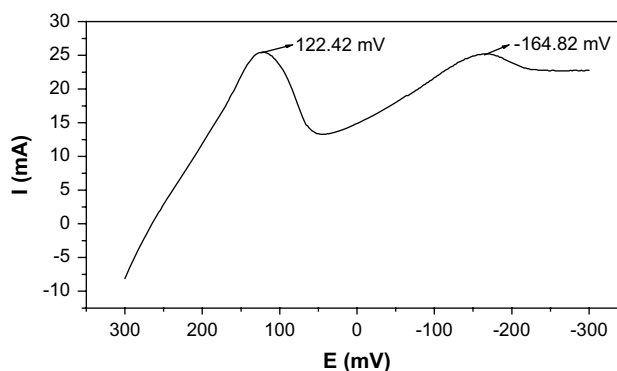


Fig. 8 – Linear sweep voltammogram with $\text{Ag}_2\text{O-Dy}_2\text{O}_3$ mixture as catalyst.

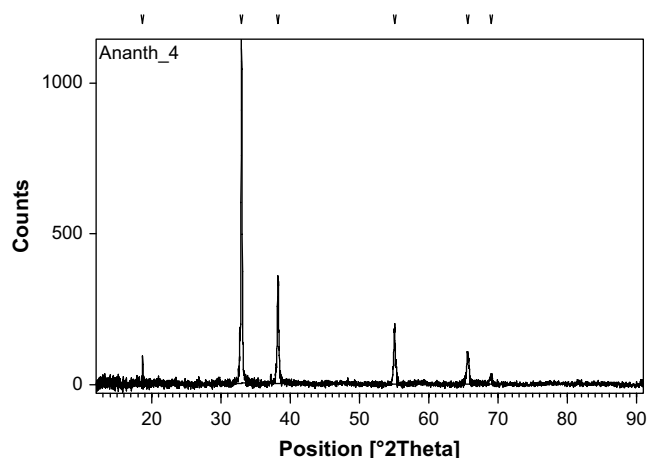


Fig. 9 – XRD pattern of the promising Ag_2O catalyst.

reaction. The results are presented in Figs. 6–8. The oxygen reduction potentials are seen around -126 mV for $\text{Ag}_2\text{O}-\text{MnO}_2$. The oxygen reduction potentials are seen around 157 and -57 mV for $\text{Ag}_2\text{O}-\text{Sm}_2\text{O}_3$. The oxygen reduction potentials are seen around 122 and -164 mV for $\text{Ag}_2\text{O}-\text{Dy}_2\text{O}_3$. The onset potential and the magnitude of the current for oxygen reduction differ from sample to sample. Obviously, the mechanism of oxygen reduction on different samples is different. The inference is that due some shift towards positive values of oxygen reduction potentials, these mixture

combinations show some promise as materials for use in air electrode. It might be that formation of some solid-state redox couple contributes to the improvement obtained with such mixtures. It is also seen that occurrence of oxygen reduction potential at the minimally negative voltage values results in superior oxygen reduction. Some reports indicate that electrocatalytic activity of the oxide towards ORR greatly increases when it is used in the form of composite electrode rather than in the form of a non-composite electrode [38]. The observed improvement could also be due to increased Ag reactivity or Ag d-band for producing stronger Ag–O interactions, leading to easier O–O bond breaking and, consequently, enhancing the ORR kinetics [44]. In addition, it is worthwhile to note that whereas Ag oxides are inactive for the ORR, Ag hydroxides are active [40]. Hence prudence in the identification of appropriate mixture combinations is required.

3.1.7. ORR peak potential and current

Different surface processes may lead to different ORR peak potentials and ORR peak currents. The appearance of the ORR peak is caused by the deficiency of the reactant on the electrode surface. When the potential decreases the electron transfer ability of the electrode increases and the current increases accordingly. However, the current will not increase further because of the shortage of the reactant on the electrode surface, i.e., limitation by transfer. Since the oxygen concentration remains constant in all the experiments, the ORR peak potential is determined by the relative rate of diffusion and surface reaction. The more positive ORR peak

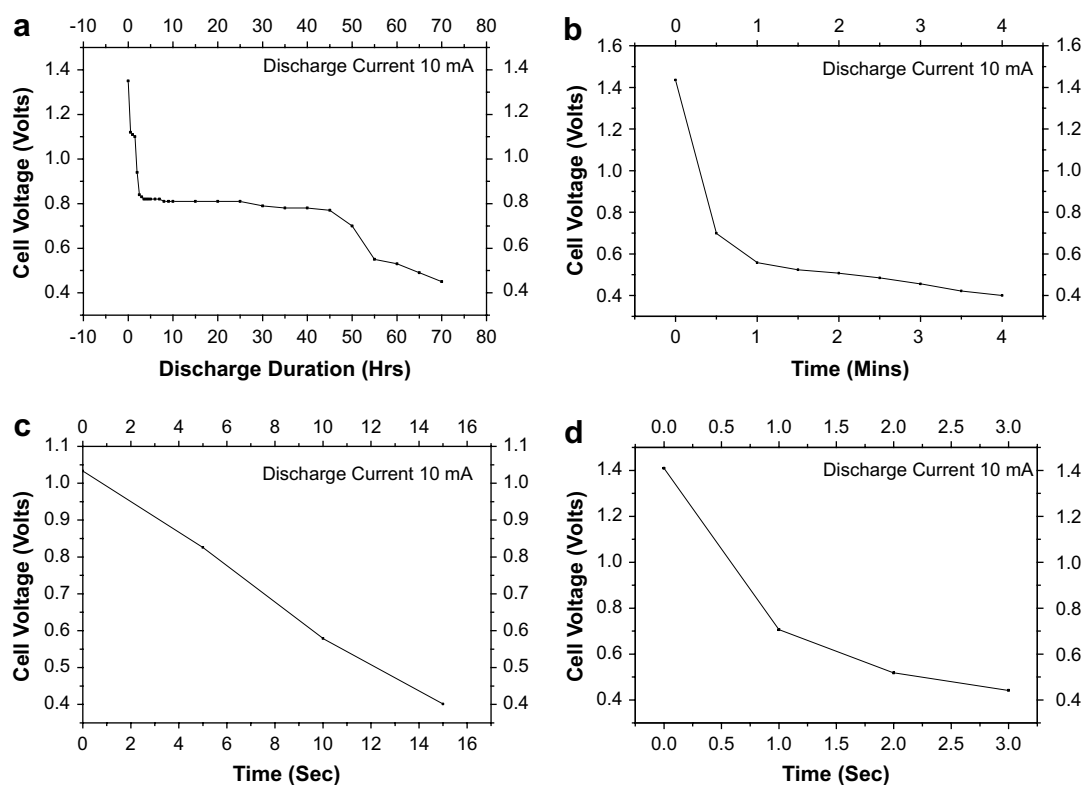


Fig. 10 – (a) Discharge curve of air–MH cell with Ag_2O as catalyst in air electrode. (b) Discharge curve of air–MH cell with MnO_2 as catalyst in air electrode. (c) Discharge curve of air–MH cell with Dy_2O_3 as catalyst in air electrode. (d) Discharge curve of Air–MH cell with Sm_2O_3 as catalyst in air electrode.

potential of Ag_2O can be attributed to its higher catalytic activity of oxygen reduction than those of the other samples.

3.2. XRD investigations

In addition to the electrochemical experiments, the XRD pattern of the promising Ag_2O catalyst was measured and is given in Fig. 9. It is seen that the observed peaks are characteristic of Ag_2O .

3.3. Charge/discharge experiments

The discharge curves of the assembled air–MH cells are shown in Fig. 10(a–d). Reasonably good performance is seen in only in Ag_2O . It is found that the other investigated materials are not useful, as they give only dismal capacity output. Particularly the undesirable crystalline structure in the engaged MnO_2 could be responsible for the observed dismal performance.

4. Conclusions

LSV investigations are performed on some oxides/mixtures to observe the efficiency of oxygen reduction. The oxygen reduction potential for the best performing Ag_2O electrode occurs at -60.67 mV. The oxygen reduction potentials for MnO_2 , Sm_2O_3 , NdO_2 and Dy_2O_3 electrodes are -270.31 , -111 , -158.58 and -130.24 mV, respectively. Evaluation of Air–MH cells using some of the above investigated oxides as catalyst for air electrode indicate that the performance is the maximum with Ag_2O as electrocatalyst amongst the studied materials. Ag_2O – MnO_2 (oxygen reduction peaks at -126 mV), Ag_2O – Sm_2O_3 (oxygen reduction peaks at 156.8 , -56.86 mV) and Ag_2O : Dy_2O_3 (oxygen reduction peaks at 122.42 , -164.82 mV) equal mixtures show some promise by showing shift in occurrence of ORR at comparatively more positive potentials and increased peak currents. Improvement and optimization are envisioned in such oxide mixtures. The LSV findings are in accordance with air–MH cell performance. Silver oxide-based materials are identified as suitable electrocatalysts for air electrode by virtue of their occurrence of ORR potentials.

Acknowledgement

The authors thank the Director, CECRI, Karaikudi for encouragement and permission to publish this work. Thanks are to MNES, New Delhi for sanctioning a Grant-In-Aid project on 'Development of Advanced Ni–MH Battery fitted Electric Cycle and Field Studies' in extension of which the above work has been done. The authors also thank Dr. G. Balachandran, DMRL, Hyderabad, India, for preparing the MH alloy. The authors would like to express their gratefulness to Dr. N.G. Renganathan and Dr. V. Yegnaraman, Division Heads, CECRI for providing necessary facilities. Sincere thanks are extended to M. Raju and K. Manimaran, scientists of Ni–MH Section for valuable suggestions and help in conducting experiments. One of the authors, KR, thank the Director, CECRI for

permission to carry out her MSc. project work and Dr. MVA for guidance.

REFERENCES

- [1] Holze R, Vielstich W. The kinetics of oxygen reduction at porous teflon-bonded fuel cell electrodes. *J Electrochem Soc* 1984;131(10):2298–303.
- [2] Walton CW, Rudd EJ, editors. Energy and electrochemical processing for a cleaner environment, vol. 97–28. Pennington, NJ: The Electrochemical Society; 1997. p. 129.
- [3] Arai H, Muller S, Haas O. AC impedance analysis of bifunctional air electrodes for metal–air batteries. *J Electrochem Soc* 2000;147(10):3584–91.
- [4] Zheng J-S, Zhang X-S, Li P, Zhou X-G, Yuan W-K. Microstructure effect of carbon nanofiber on electrocatalytic oxygen reduction reaction. *Catal Today* 2008;141(1–4):270–7.
- [5] Wang P, Ma Z, Zhao Z, Jia L. Oxygen reduction on the electrocatalysts based on pyrolyzed non-noble metal/poly-*o*-phenylenediamine/carbon black composites: new insight into the active sites. *J Electroanal Chem* 2007;611(1–2):87–95.
- [6] Sarapuu A, Helstein K, Schiffrin DJ, Tammeveski K. Kinetics of oxygen reduction on quinone-modified HOPG and BDD electrodes in alkaline solution. *Electrochem Solid-State Lett* 2005;8(2):E30–3.
- [7] Maruyama J, Abe I. Cathodic oxygen reduction at the interface between Nafion® and electrochemically oxidized glassy carbon surfaces. *J Electroanal Chem* 2002;527(1–2): 65–70.
- [8] Yano T, Popa E, Tryk DA, Hashimoto K, Fujishima A. Electrochemical behavior of highly conductive boron-doped diamond electrodes for oxygen reduction in acid solution. *J Electrochem Soc* 1999;146(3):1081–7.
- [9] Friedrich JM, Poncedeleón C, Reade GW, Walsh FC. Reticulated vitreous carbon as an electrode material. *J Electroanal Chem* 2004;561(1):203–17.
- [10] Britto PJ, Santhanam KSV, Rubio A, Alonso A, Ajayan PM. Improved charge transfer at carbon nanotube electrodes. *Adv Mater* 1999;11(2):154–7.
- [11] Bessel CA, Laubernds K, Rodriguez NM, Baker RTK. Graphite nanofibers as an electrode for fuel cell applications. *J Phys Chem B* 2001;105(6):1115–8.
- [12] Ambrosio EP, Francia C, Manzoli M, Penazzi N, Spinelli P. Platinum catalyst supported on mesoporous carbon for PEMFC. *Int J Hydrogen Energy* 2008;33(12):3142–5.
- [13] Bockris JO'M. Will lack of energy lead to the demise of high-technology countries in this century? *Int J Hydrogen Energy* 2007;32(2):153–8.
- [14] Garsuch A, Yang R, Bonakdarpour A, Dahn JR. The effect of boron doping into Co–C–N and Fe–C–N electrocatalysts on the oxygen reduction reaction. *Electrochim Acta* 2008;53(5): 2423–9.
- [15] Jahnke H, Schönborn M, Zimmermann G. Organic dyestuffs as catalysts for fuel cells. *Top Curr Chem* 1976;61:133–81.
- [16] Jasinski R. A new fuel cell cathode catalyst. *Nature (London)* 1964;201:1212–3.
- [17] Scherson D, Tanaka AA, Gupta SL, Tyrk D, Fierro C, Holze R, et al. Transition metal macrocycles supported on high area carbon: pyrolysis–mass spectrometry studies. *Electrochim Acta* 1986;31(10):1247–58.
- [18] Wiesener K. N_4 -chelates as electrocatalyst for cathodic oxygen reduction. *Electrochim Acta* 1986;31(8):1073–8.
- [19] Antolini E, Salgado JRC, Giz MJ, Gonzalez ER. Effects of geometric and electronic factors on ORR activity of carbon supported Pt–Co electrocatalysts in PEM fuel cells. *Int J Hydrogen Energy* 2005;30(11):1213–20.

- [20] Castellanos RH, Ocampo AL, Moreira-Acosta J, Sebastian PJ. Synthesis and characterization of osmium carbonyl cluster compounds with molecular oxygen electroreduction capacity. *Int J Hydrogen Energy* 2001;26(12):1301–6.
- [21] Arico AS, Srinivasan S, Antonucci V. DMFCs: from fundamental aspects to technology development. *Fuel Cells* 2001;1:133–61.
- [22] Chan KY, Ding J, Ren JW, Cheng SA, Tsang KY. Supported mixed metal nanoparticles as electrocatalysts in low temperature fuel cells. *J Mater Chem* 2004;14:505–16.
- [23] Loffler MS, Gro B, Natter H, Hempelmann R, Krajewski T, Divisek J. Synthesis and characterization of catalyst layers for direct methanol fuel cell applications. *Phys Chem Chem Phys* 2001;3:333–6.
- [24] Lima A, Coutanceau C, Leger JM, Lamy C. Investigation of ternary catalysts for methanol electrooxidation. *J Appl Electrochem* 2001;31(4):379–86.
- [25] Wang B. Recent development of non-platinum catalysts for oxygen reduction reaction. *J Power Sources* 2005;152:1–15.
- [26] Lopes T, Antolini E, Gonzalez ER. Carbon supported Pt–Pd alloy as an ethanol tolerant oxygen reduction electrocatalyst for direct ethanol fuel cells. *Int J Hydrogen Energy* 2008;33(20):5563–70.
- [27] De Koninck M, Manseau P, Marsan B. Preparation and characterization of Nb-doped TiO₂ nanoparticles used as a conductive support for bifunctional CuCo₂O₄ electrocatalyst. *J Electroanal Chem* 2007;611(1–2):67–79.
- [28] Hu WK, Ye Z, Noreus D. Influence of MH electrode thickness and packing density on the electrochemical performance of air–MH batteries. *J Power Sources* 2001;102(1–2):35–40.
- [29] Chartouni D, Kuriyama K, Kiyobayashi T, Chen J. Air–metal hydride secondary battery with long cycle life. *J Alloy Compd* 2002;330–332:766–70.
- [30] Mohamad AA, Mohamed NS, Alias Y, Arof AK. Mechanically alloyed Mg₂Ni for metal–hydride–air secondary battery. *J Power Sources* 2003;115(1):161–6.
- [31] Chartouni D, Kuriyama N, Kiyobayashi T, Chen J. Metal hydride fuel cell with intrinsic capacity. *Int J Hydrogen Energy* 2002;27(9):945–52.
- [32] Mao L, Zhang D, Sotomura T, Nakatsu K, Koshiha N, Ohsaka T. Mechanistic study of the reduction of oxygen in air electrode with manganese oxides as electrocatalysts. *Electrochim Acta* 2003;48(8):1015–21.
- [33] Yang C-C. Preparation and characterization of electrochemical properties of air cathode electrode. *Int J Hydrogen Energy* 2004;29(2):135–43.
- [34] Verma A, Jha AK, Basu S. Manganese dioxide as a cathode catalyst for a direct alcohol or sodium borohydride fuel cell with a flowing alkaline electrolyte. *J Power Sources* 2005;141(1):30–4.
- [35] Yang C-C, Hsu S-T, Chien W-C, Chang Shih M, Chiu S-J, Lee K-T. Electrochemical properties of air electrodes based on MnO₂ catalysts supported on binary carbons. *Int J Hydrogen Energy* 2006;31(14):2076–87.
- [36] Burchardt T. An evaluation of electrocatalytic activity and stability for air electrodes. *J Power Sources* 2004;135(1–2):192–7.
- [37] Chang C-C, Wen T-C. Kinetics and mechanism of oxygen reduction at hydrous oxide film-covered platinum electrode in alkaline solution. *Electrochim Acta* 2006;52(2):623–9.
- [38] Singh RN, Malviya M, Anindita, Sinha ASK, Chartier P. Polypyrrole and La_{1-x}Sr_xMnO₃ (0 ≤ x ≤ 0.4) composite electrodes for electroreduction of oxygen in alkaline medium. *Electrochim Acta* 2007;52(12):4264–71.
- [39] Ananth MV, Manimaran K, Arul Raj I, Sureka N. Influence of air electrode electrocatalysts on performance of air–MH cells. *Int J Hydrogen Energy* 2007;32(17):4267–71.
- [40] Demarconnay L, Coutanceau C, Léger J-M. Electroreduction of dioxygen (ORR) in alkaline medium on Ag/C and Pt/C nanostructured catalysts—effect of the presence of methanol. *Electrochim Acta* 2004;49(25):4513–21.
- [41] Wagner N, Schulze M, Gülzow E. Long-term investigations of silver cathodes for alkaline fuel cells. *J Power Sources* 2004;127(1–2):264–72.
- [42] Obradović MD, Grgur BN, Vračar LM. Adsorption of oxygen containing species and their effect on oxygen reduction on Pt₃Co electrode. *J Electroanal Chem* 2003;548:69–78.
- [43] Li YJ, Chang CC, Wen TC. A mixture design approach to thermally prepared Ir–Pt–Au ternary electrodes for oxygen reduction in alkaline solution. *J Appl Electrochem* 1997;27(2):227–34.
- [44] Lima FHB, de Castro JFR, Ticianelli EA. Silver–cobalt bimetallic particles for oxygen reduction in alkaline media. *J Power Sources* 2006;161(2):806–12.
- [45] Zheng J-S, Zhang X-S, Li P, Zhou X-G, Chen D, Liu Y, et al. Oxygen reduction reaction properties of carbon nanofibers: effect of metal purification. *Electrochim Acta* 2008;53(10):3587–96.
- [46] Lima FHB, Calegario ML, Ticianelli EA. Investigations of the catalytic properties of manganese oxides for the oxygen reduction reaction in alkaline media. *J Electroanal Chem* 2006;590(2):152–60.
- [47] Burke LD, Casey JK, Morrissey JA. An investigation of some of the variables involved in the generation of an unusually reactive state of platinum. *Electrochim Acta* 1993;38(7):897–906.